ISSN 1068-3666, Journal of Friction and Wear, 2023, Vol. 44, No. 6, pp. 367–375. © Allerton Press, Inc., 2023.
Russian Text © The Author(s), 2023, published in Trenie i Iznos, 2023, Vol. 44, No. 6, pp. 551–561.

Determination of the Carrying Ability of Metal-Fluoroplast Slide Bearings Using the Finite Element Method

K. Yu. Zershchikov[a], *, A. S. Yelkin[b], I. V. Sergeichev[b], Yu. V. Semenov[a], and A. V. Mashkov[a]

[a] *Constant-2 LLC, Volgograd oblast, Volgograd, 400120 Russia*

[b] *Institute of Science and Technology, Moscow, 121205 Russia*

**e-mail: secret@constanta-2.ru*

Received July 24, 2023; revised November 28, 2023; accepted December 12, 2023

Abstract—Based on the proposed loading model of a sliding bearing, the dependence of the load-bearing capacity of reinforced metal fluoroplastic sliding bearings on their geometric characteristics and force factors was studied using the finite element method. A calculation of stresses and deformations in the most pliable antifriction layer was carried out. It is shown that the distribution of stresses and deformations in the bearing is extremely uniform and depends on the thickness of the antifriction layer and the height of the bearing. Criteria for assessing the performance of sliding bearings under load were introduced and based on these criteria the results were compared with experimental data. The agreement between calculated and experimental data allows us to use the resulting methodology to determine the load-bearing capacity of slide bearings. The solutions make it possible to move from the experimental method of determining the load-bearing capacity of metal fluoroplastic sliding bearings to the calculated one and to design bearings with predetermined strength characteristics. This will help specialists designing bearing units improve the quality and speed of their development.

Keywords: metal-fluoroplast slide bearing, finite element modeling, calculations of stress and strain, antifriction layer, computation, carrying ability

DOI: 10.3103/S1068366623060119

INTRODUCTION

Metal-polymer slide bearings (MPSBs) have been long and widely used in mechanical engineering due to their well-known advantages: high load-bearing capacity, the ability to operate without lubrication, insensitivity to temperature fluctuations, and excellent weight and size characteristics [1]. The emergence of new materials makes it possible to develop new design and technological solutions and achieve higher performance characteristics. The intensification of production processes, transition to high operating parameters, and the expansion of the areas of application of MPSBs require the presence of a reliable apparatus for predicting their properties. All this makes it necessary to have verified methods for calculating and designing bearings for their justified use, and to solve emerging problems on this basis.

The existing methodology for calculating the strength of slide bearings is based on expert and experimental assessment of their load-bearing capacity. It is based on comparison of the average pressure, defined as the difference between the force acting on the bearing and its nominal area, equal to the product of the internal diameter and the height of the bearing with the permissible strength value, established, as mentioned earlier, on the basis of experimental data, operating experience, and expert assessments.

Thus, for metal fluoroplastic bearings, the average pressure under static loading is taken within the range of 250–400 MPa, depending on the design of the bearing [1, 9]. For other types of loads, in particular at frequent alternating effects of pressure and speed, a reduction factor to these values is introduced, equal to $K = 2–3$. As noted in [1], when choosing slide bearings, a verification calculation is carried out, based on the specified dimensions and physicomechanical properties of the bearing materials, as well as operating parameters. Load-bearing capacity and durability in hours or cycles are tested. According to [2], the elements of bushings subject to evaluation are thickness δ, length l, and energy parameter PV, where V is the speed of mutual movement. In this case, $\delta = (0.03–0.06)D$ is accepted, where D is the shaft diameter. In [3], it is recommended to assign H and δ based on the ratio $H/\delta < 25$. For bearings, subjected to static loading in [3, 4], the ratio $H = (1–1.2)D$ is recommended. Thus, existing methods used to design self-lubricating slide bearings do not take into account the real stress-strain state (SSS) realized in bearings under loading. Therefore, it is necessary to create an adequate model

Table 1. Properties of the materials used in the calculation

Property	Base—steel 08ps	Anti-friction layer—reinforced fluoroplastic
Tensile yield strength, MPa	200	160
Relative elongation at break, %	20	5
Modulus of elasticity, MPa	200000	2000
Poisson's ratio	0.30	0.35
Coefficient of dry sliding friction of fluoroplastic on steel	0.05	
Deformation, onset of yield, %	1	10

for calculating stresses and deformations of bearings and assessing the bearing capacity of the MPSB.

In [8–12], attempts to use the finite element method to determine the performance of slide bearings have been made. However, most studies focus on calculating the wear rate depending on external factors, and pressure on the bearing is calculated based on solving known contact problems. At the same time, the SSS of a material largely determines its behavior under load, including its wear characteristics.

Objective—To evaluate the possibility of using the finite element method to calculate the load-bearing capacity of MPSBs.

FORMULATION OF THE PROBLEM

As noted earlier, the variety of used materials and design solutions for bearings require justification for their use for certain operating conditions. The main external factors affecting the bearing are pressure in pairing P, temperature T, at which the bearing is operated, speed of mutual movement V, and the energy or PV factor—the product of the pressure acting in the bearing assembly and the speed of mutual movement of the pairing surfaces. The main design characteristics of MPS radial bearings are diameter, height, thickness, and layer materials. Obviously, the task of the calculation is to determine the influence of all these factors on the bearing capacity and durability of the bearings.

One of the most important conditions for strength calculations is the setting of limit values and values, the excess of which will lead to loss of performance of the bearing assembly, that is, setting the parameters of the limit state. As established in [5], a change in the pairing gap by more than 0.1 mm is taken as this value; in fact, this is a decrease in the thickness of the bearing as a result of plastic deformation or wear by more than 0.1 mm; a condition for limiting deformations. This value is the limit for the normal functioning of the MPSB. In [6], the limit deformation is given as 0.25 mm. Probably, different values of the critical gap in the joint are due to differences in estimates of the durability associated with it, however, we will be guided by a more conservative value of 0.1 mm. It is also obvious that the operation of the bearing is possible when the stresses do not exceed the yield strength or strength of the material; conditions of yield strength. The above conditions can be written as:

$$\frac{\varepsilon_y}{\varepsilon} > 1 \quad \text{and} \quad \frac{\sigma_y}{\sigma} > 1, \tag{2}$$

where ε_y and σ_y are the limiting values, and ε and σ are the acting values of deformation and stress.

Consequently, the criteria for the limit state will be considered to be bearing deformation greater than a critical value and (or) internal stresses, exceeding strength characteristics of the materials. Thus, the task of the calculation is to determine stresses and deformations acting in the bearing under the influence of external force and temperature factors, and given geometric characteristics of the bearing, compare them with the limiting values. The initial data for calculating stresses and strains to determine the performance of the bearing based on criteria (2) are presented in Table 1.

SIMULATION RESULTS

The calculation was carried out using the Abaqus software package. The calculation is based on a loading scheme that corresponds to the experimental setup diagram described in [7] and shown in Fig. 1a. The following provisions were introduced in the calculations: (a) the bearing is a continuous bushing and is considered as a two-layer composite, the layers of which have excellent properties and are adhesively connected with a known value of adhesive strength: the outer layer is steel 08ps with a thickness from 0.8 to 2.3 mm, the anti-friction layer is a composite material F-4 fluoroplastic reinforced with glass fiber with a thickness from 0.1 to 0.5 mm; (b) the calculation is nonlinear; (c) the properties of materials are determined by the deformation curves of an ideal elastic-plastic body; (d) to increase the accuracy in the calculation, the quadratic type of elements has been used; (e) fastenings and torque are transmitted to the shaft using Coupling elements; and (f) there is no gap in the joint.

The loading diagram and dimensions of the bearing and supports are shown in Fig. 1a. Bearing (*3*) is

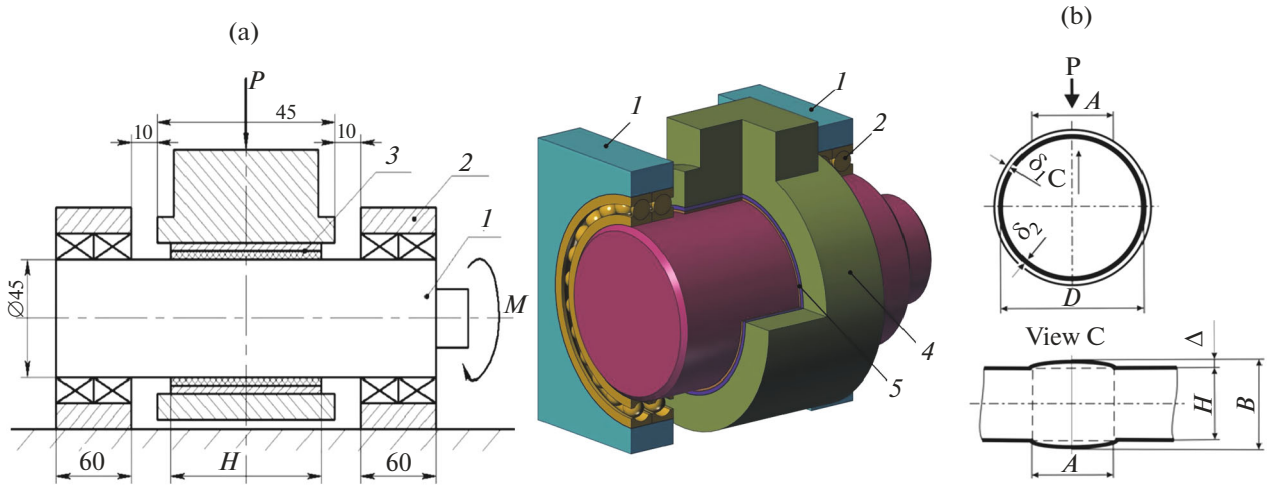

Fig. 1. Scheme of the experimental unit (a) and scheme for measuring geometric dimensions after testing (b).

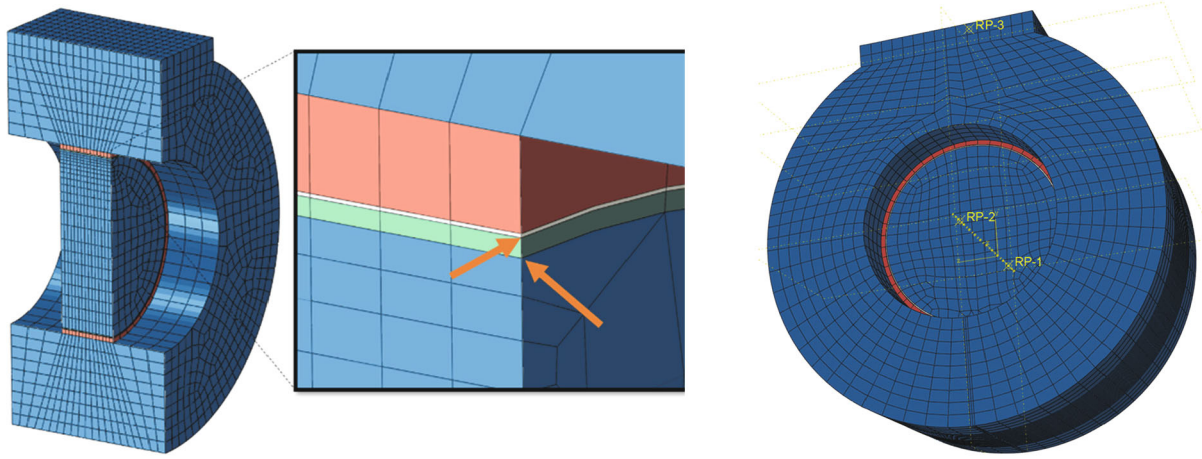

Fig. 2. The size and nature of the grid for the calculation model of a metal-fluoroplast slide bearing.

installed on shaft (*1*) with a diameter of 45 mm, and load *P* is transmitted to it through massive housing (*4*). Since the diameter of the shaft, as a rule, is set from the strength calculation of the structure or assembly, into which the bearing is installed, the bearing height and thickness of the layers must be determined from the strength conditions. During the experiment (and calculation), pressure *P* was varied, as well as height *H* and thickness δ of the bearing and their change under the influence of changing pressure.

Figure 2 shows the finite element method of the bearing assembly (the shaft is shown in fragments).

Since the modulus of elasticity of the antifriction layer is two orders of magnitude lower than that of steel, it is obvious to assume that it will make the main contribution to the deformation of the bearing under load. As confirmation, Fig. 3 shows the calculated relative deformations of the steel base and the anti-friction layer, from which it can be seen that the value of the relative deformation of the steel base is almost two orders of magnitude less—0.5% than the anti-friction layer—28%. Therefore, and also due to the fact that namely it provides the main functions of the MPSBs, in the future, the main attention will be paid to the analysis of the stress-strain state of the antifriction layer.

Figure 4 shows the equivalent stresses in the anti-friction layer when the bearing height changes at the same average pressure of 230 MPa. As can be seen, the value of the equivalent stress is 150 MPa and is practically independent of the bearing height and is below the average pressure of 230 MPa. This means that the stresses in the antifriction layer do not exceed the yield

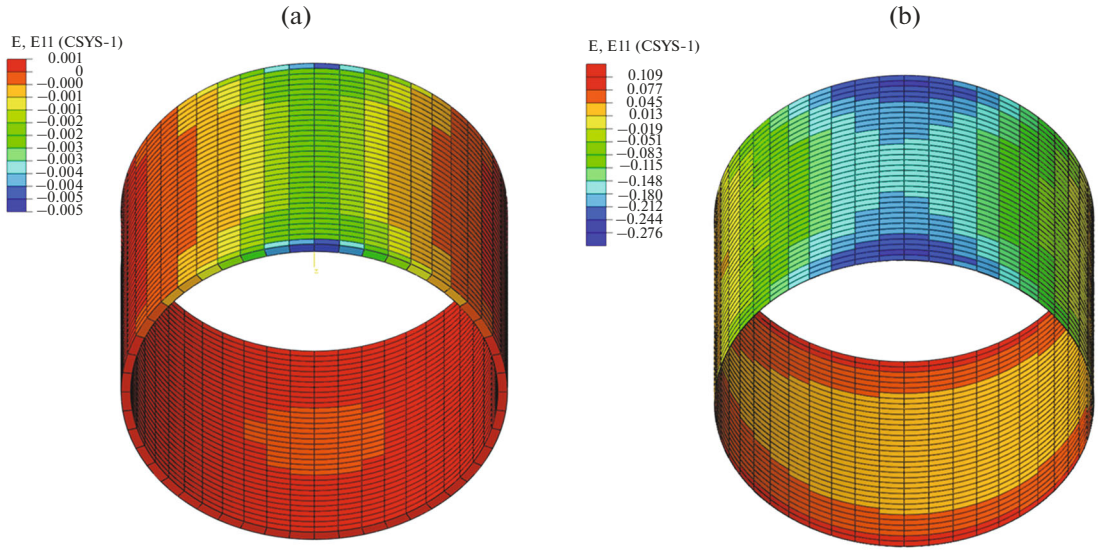

Fig. 3. Comparison of strains of the steel base (a) and the antifriction layer (b) at a load of 230 MPa.

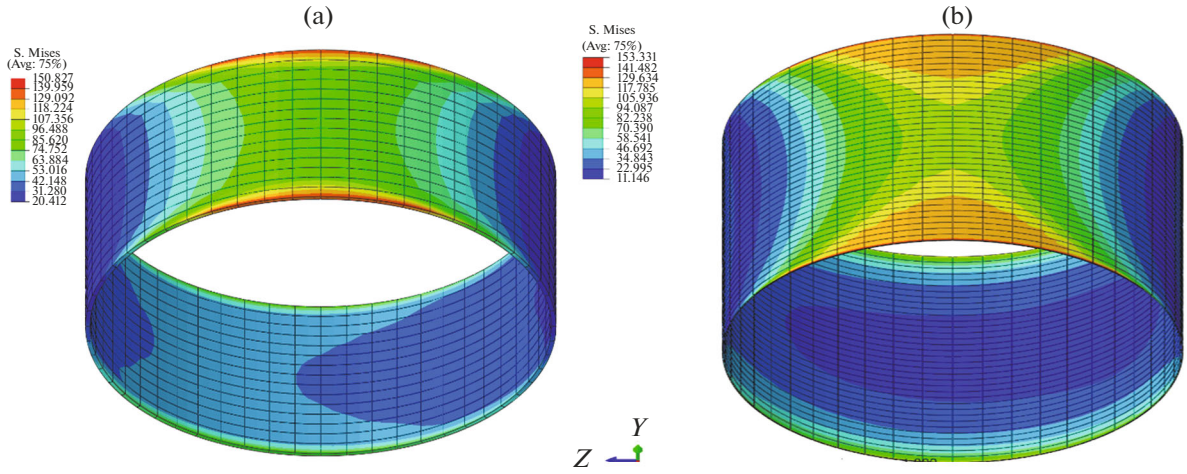

Fig. 4. Equivalent stress in an anti-friction layer 0.3 mm thick when the bearing height changes: (a) 15 mm; (b) 35 mm. Average pressure 230 MPa.

strength of the material. As expected, the stresses are maximum at the top of the bearing and decrease as they move from the top to the equator. The stress distribution changes with increasing height: with a bearing height of 15 mm, a high stress gradient is observed, when moving from the edge to the center (Fig. 4a); at a length of 1 mm, the stresses decrease from 150 to 100 MPa, while for a bearing with a height of 35 mm, the length of this zone is 10 mm (Fig. 4b). The observed picture is explained by an increase in the amount of shaft deflection under load as the bearing height increases from 15 to 35 mm.

Changing the thickness of the antifriction layer from 0.15 to 0.5 mm at fixed average pressure of 230 MPa has virtually no effect on the value of the maximum stress acting in the antifriction layer (Fig. 5). The width of the zone of action of maximum stresses of 150 MPa and the stress gradient during the transition from the edge to the center increase with increasing the thickness of the deformable layer, but the stress distribution pattern does not change significantly.

The presence of low stresses (~20 MPa) in the lower, virtually unloaded part of the bearing, is an unexpected

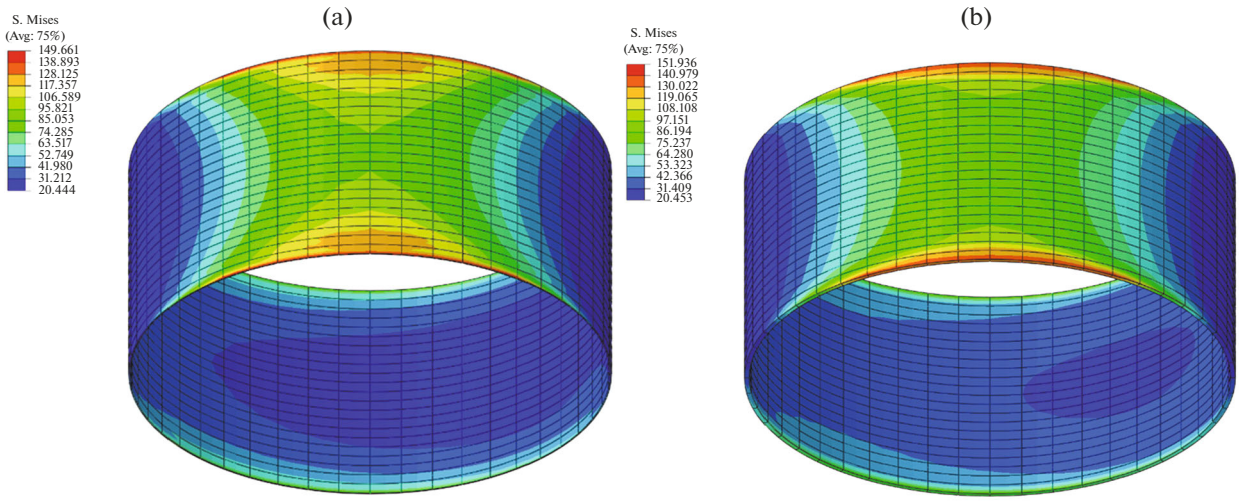

Fig. 5. Change of stress state when changing the thickness of the antifriction layer from 0.15 (a) to 0.5 mm (b). $H = 22$ mm. Average pressure 230 MPa.

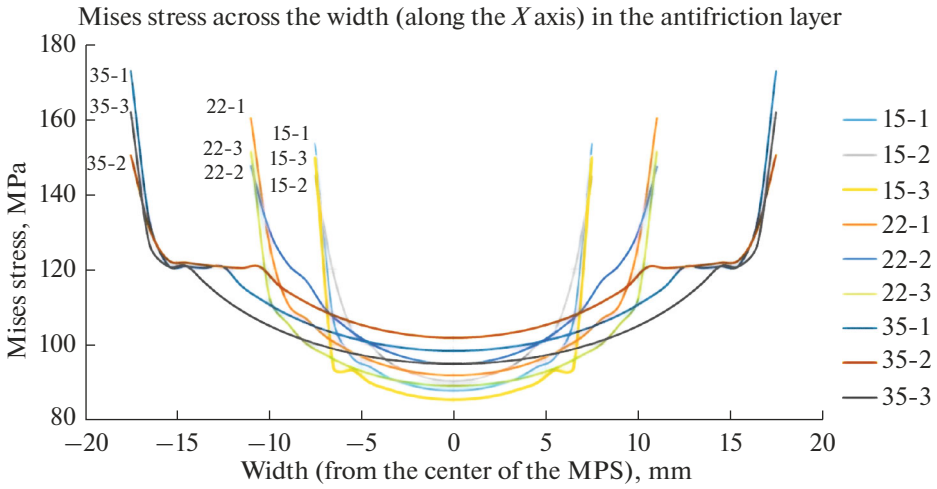

Fig. 6. Influence of bearing geometric characteristics on stresses in the antifriction layer: 15, 22, 35—bearing height in mm; 1, 2, 3—layer thickness 0.3, 0.15, and 0.5 mm, respectively.

result, but, as a refined calculation showed, it is explained by the assumption that there is no gap in the joint. The calculation results showed that no significant change in the stress-strain state is observed.

Figure 6 shows a generalized graph of the influence of geometric parameters on the stress state of the bearing obtained from the calculations. There is a weakly expressed dependence of the maximum equivalent stresses on the bearing height. As the height of the bearing increases by more than 2 times, the stress level in the antifriction layer increases by no more than 15%. The effect of the thickness of the antifriction layer on stresses is ambiguous, but in general, a change in the thickness of more than 3 times also changes the stress by no more than 15%. Let us note the uneven distribution of stresses along the height: the stresses at the edges of the bearings are almost 2 times higher than the stresses in the central part, which we associate with the deflection of the shaft under load. Thus, the calculation shows a insignificant influence of geometric characteristics of the bearing on the stressed state of the antifriction layer. At the same time, there is a combined effect of thickness and height on the stress state of the antifriction layer (Fig. 6), which once again confirms the need to take into account all factors upon designing bearings. It is important that at all studied options, the effective stresses do not exceed the yield strength of the material, that is, the limit state is not reached, and the bearing remains operational.

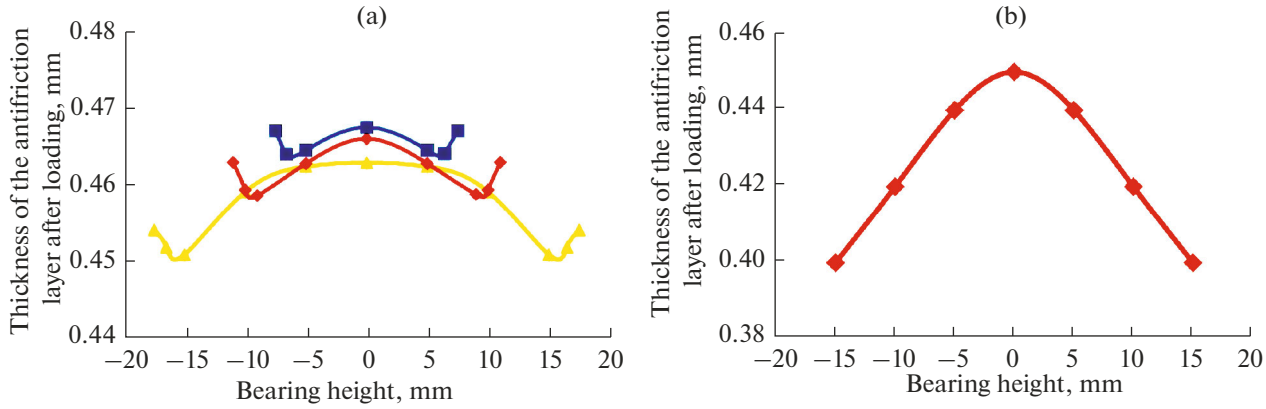

Fig. 7. Strain distribution over the height of the antifriction layer with a change in its thickness and bearing height and comparison of calculated (H = ▲ 35, ◆ 22, and ■ 15 mm) (a) and experimental (◆ H = 30 mm) (b) dependences. Initial thickness 0.5 mm. Pressure 230 MPa.

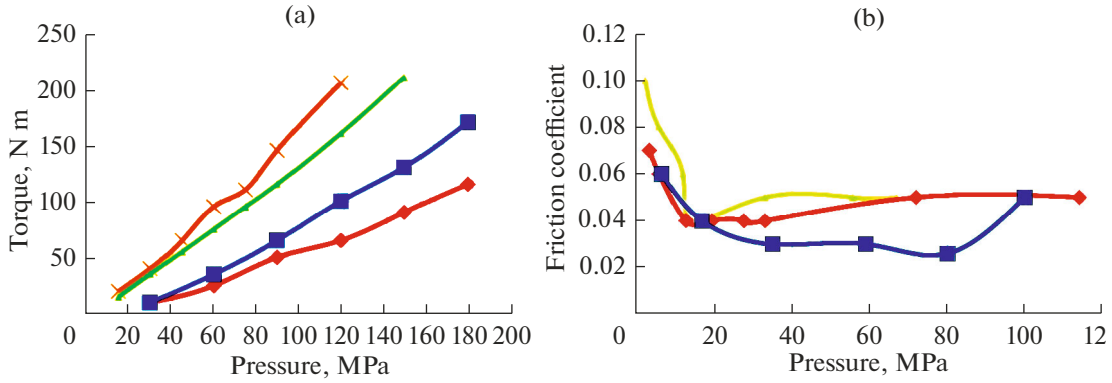

Fig. 8. Dependence of torque on applied pressure (a): ▲ H = 30 mm, δ_2 = 0.5 mm, ◆ H = 15 mm, δ_2 = 0.5 mm; ■ H = 15 mm, δ_2 = 0.1 mm; × H = 30 mm, δ_2 = 0.1 mm and friction coefficients at different pressures for bearings of different heights (b): δ_2 = 0.5 mm, H = ▲ 30, ◆ 20, and ■ 10 mm.

Let us consider the influence of geometric characteristics of the bearing on the deformation of the antifriction layer under load. Figure 7a shows the calculated dependence of the deformation of the antifriction layer in the bearing, when its height changes. It is obvious that the absolute value of the deformation increases with increasing height and reaches a maximum at the edges of the bearing. The difference between the maximum and minimum deformations also increases when moving from narrow to wide bearings. An increase in the thickness of the antifriction layer naturally leads to an increase in the absolute value of the deformation, therefore, it is undesirable from the point of view of compliance with the limiting deformation criterion. As can be seen from the comparison of Figs 7a and 7b, there is good agreement between the calculated and experimental data: the difference does not exceed 10%. In this case, the maximum absolute deformation does not exceed 0.1 mm, which indicates that criterion (3) is met, and the bearing's load-bearing capacity is maintained at the given average pressure.

EXPERIMENTAL VERIFICATION

Experimental testing was carried out on a previously described installation (Fig. 1a). The load on the bearing was set on an IP-1000 press with an accuracy of ±3 kN, the torque was measured with a dynamometer with an accuracy of ±10 N m. Linear dimensions were measured with a tool with a division value of 0.01 mm. The effect of a statically applied load and torque during shaft rotation on the deformation of the antifriction layer was checked, which was assessed by changes in its thickness and width of the deformation zone (Fig. 1b). Figure 8a shows the dependence of the rotation torque on the pressure applied to the bearing. Based on these data, friction coefficients were determined at different pressures for bearings of different heights (Fig. 8b). The value of the friction coefficient, as can be seen, is practically independent of the pressure on the bearing (within the accuracy of the experiment) and correlates well with the data in Table 1. Higher values at low pressures are explained by the running-in period.

Table 2. Bearing test results at different pressures

Thickness of steel base, mm	Antifriction layer thickness, mm	Bearing thickness before testing H, ±0.01 mm	Bearing thickness after testing H_1, ±0.01 mm	Pressure, ±0.5 MPa	Calculated stress in the layer, MPa	Height before test H, mm	$(B-H)$, mm after test	$(H-H_1)$, mm
0.7	0.3	1.02	1.02	180	120	15	0	0
		1.01	1.01	250	150	15	0.3	0
		1.03	0.99	400	170	15	1.8	0.04
		1.02	0.99	180	130	30	0.5	0.03
		1.04	1.02	250	170	30	0.8	0.02
		1.03	0.99	400	210	30	3	0.04
1	0.1	1.08	1.08	180	115	15	0	0
		1.1	1.09	250	140	15	0	0.01
		1.1	1.09	400	160	15	0	0.01
		1.1	1.1	180	125	30	0	0
		1.09	1.09	250	165	30	0	0
		1.1	1.07	400	190	30	0	0.03

Table 2 shows the results of measuring deformation of the bearings after applying a load. The calculated stresses naturally increase with increasing load P on the bearing. As can be seen, at stresses, less than the yield strength, deformations are elastic in nature, and residual deformations $(H - H_1)$ in the antifriction layer appear when the magnitudes of the acting stresses exceed the yield strength of the material $\sigma > 160$ MPa. In this case, the height of the bearing $B - H > 0$ increases due to the plastic flow of the material. Thus, the validity of the analysis of the load-bearing capacity of metal-polymer bearings based on equivalent stresses is confirmed.

Figure 9 shows the change in the stress state at various pressures applied to the MPSBs. Note that internal stresses do not grow so intensely with increasing load: when pressure changes by 3.3 times, the stresses increase by 1.7 times, and the width of the zone of increased stresses increases. In this case, stresses can reach values (190–210 MPa) exceeding the yield strength and the appearance of plastic deformations, as evidenced by the data presented in Table 2.

To check the reliability of the calculations, we tested bearings 22 mm high with an antifriction layer having a yield strength of 160 MPa at various pres-

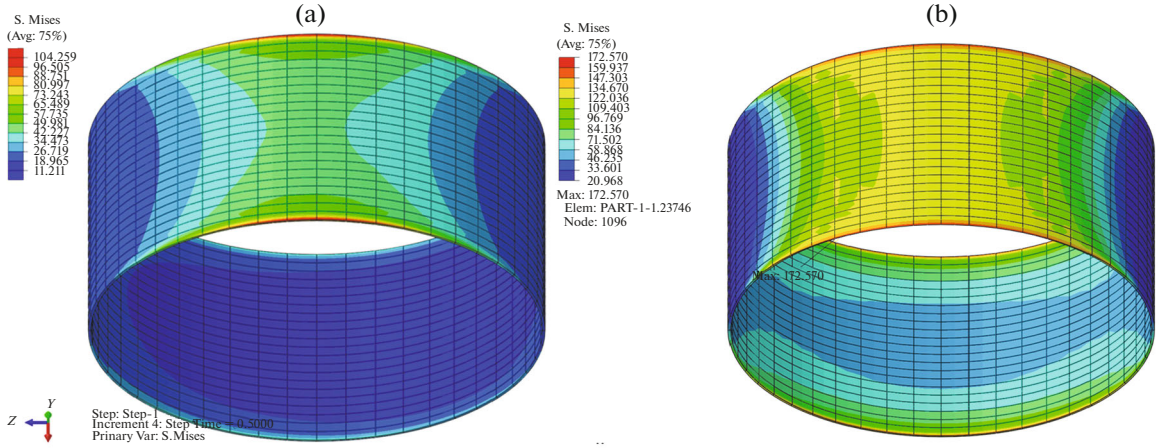

Fig. 9. Equivalent stresses in the antifriction layer at pressures of 120 (a) and 400 MPa (b). $H = 22$ mm, thickness of the antifriction layer 0.3 mm.

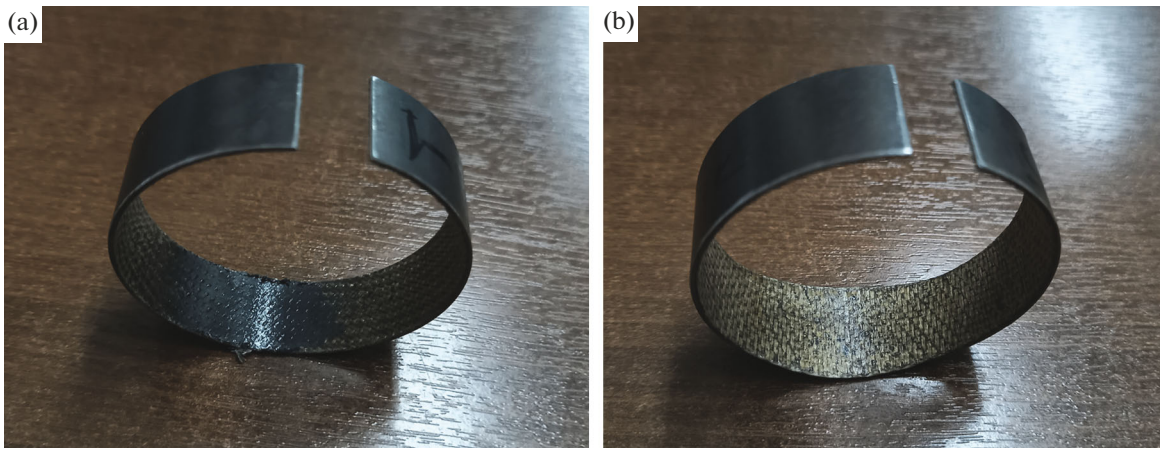

Fig. 10. Photo of sliding bearings after the test with different pressures: (a) 120; (b) 400 MPa with antifriction layer of fiberglass-reinforced fluoroplast.

sures. In Fig. 10b, the zone of plastic deformation along the edges of the bearing is clearly visible, since at a pressure of 400 MPa, the effective stresses (172 MPa) exceeded the yield strength of the material (160 MPa). At the same time, at low pressure of 120 MPa, the equivalent stresses in the antifriction layer (104 MPa) do not exceed the yield strength of the material, and no deformation is observed (Fig. 10a).

Computer simulation and experimental studies show that, knowing the standard physicomechanical properties of materials and the magnitude of the load, it is possible to calculate the strength of a bearing with given characteristics or solve the inverse problem, to develop its design for given operating conditions.

All of the above refers to strength calculations of bearings and indirectly affects the issue of their service life. However, these calculations are the starting material for moving on to more complex calculations of bearing life under dynamic loading.

CONCLUSIONS

The influence of physicomechanical characteristics of materials, thickness and height, external load on stress, and deformation in the most pliable antifriction layer of metal fluoroplastic slide bearings was studied using the finite element method. It is proposed to determine the bearing capacity by comparing the operating stresses and deformations with the permissible values. The resulting solution for calculating the load-bearing capacity of metal-polymer plane bearings allows one to move from intuitive to theoretically based decisions about the applicability of bearings. Experimental data confirmed the correctness of the provisions laid down in the calculation methodology, which allows one to move on to the design of bearings with predetermined geometric characteristics and strength properties. The resulting solutions make it possible to develop bearing units for highly loaded supports and shafts under loads of up to 400 MPa at low rotation speeds of up to 0.01 m/s.

FUNDING

The investigation has been performed with the help of the Russian scientific fund no. 21-19-00563, https://rscf.ru/project/21-19-00563.

CONFLICT OF INTEREST

The authors of this work declare that they do not have any conflicts of interest.

REFERENCES

1. Semenov, A.P. and Savinskii, Yu.E., *Metalloftoroplastovye podshipniki* (Metal-Fluoroplastic Bearings), Moscow: Mashinostroenie, 1976.
2. *Proizvodstvo izdelii iz polimernykh materialov* (Product Manufacturing from Polymer Materials), Kryzhanovskii, V.K. , Eds., St. Petersburg: Professiya, 2004.
3. Fedorchenko, I.M. and Pugina, L.I., *Kompozitsionnye, spechennye antifriktsionnye materialy* (Composition, Sintered Antifriction Materials), Kiev: Naukova Dumka, 1980.
4. Bykov, A.F., *Armatura s sharovym zatvorom dlya gidravlicheskikh sistem* (Valves with Ball Gate for Hydraulic Systems), Moscow: Mashinostroenie, 1971.
5. Zershchikov, K.Yu. and Semenov, Yu.V., Dependence of bearing capacity of metal-polymer plane bearings on their geometric characteristics, *Konstr. Kompoz. Mater.*, 2012, no. 1, pp. 28–31.
6. Zershchikov, K.Yu. and Kuzakhmetova, E.K., Metal-polymer bearings for revolution units of gate pipe fittings, *Truboprovodnaya Armatura Oborud.*, 2012, no. 2, pp. 22–23.
7. Metal/polymer composite plain bearings. https://www.schaeffler.com/remotemedien/media/_shared_-

media/08_media_library/01_publications/schaeffler_2/tpi/downloads_8/tpi_211_de_en.pdf.

8. Martínez, F.J., Canales, M., Izquierdo, S., Jiménez, M.A., and Martínez, M.A., Finite element implementation and validation of wear modelling in sliding polymer–metal contacts, *Wear*, 2012, vols. 284–285, pp. 52–64. https://doi.org/10.1016/j.wear.2012.02.003

9. Chernets, M., Chernets, J., Kindrachuk, M., and Kornienko, A., Methodology of calculation of metal-polymer sliding bearings for contact strength, durability and wear, *Tribol. Ind.*, 2020, vol. 42, no. 4, pp. 572–581. https://doi.org/10.24874/ti.900.06.20.10

10. Dykha, A., Sorokatyi, R., Makovkin, O., and Babak, O., Calculation-experimental modeling of wear of cylindrical sliding bearings, *Eastern-Eur. J. Enterpr. Technol.*, 2017, vol. 5, no. 1, pp. 51–59. https://doi.org/10.15587/1729-4061.2017.109638

11. Zernin, M.V., Mishin, A.V., Rybkin, N.N., Shil'ko, S.V., and Ryabchenko, T.V., Consideration of the multizone hydrodynamic friction, the misalignment of axes, and the contact compliance of a shaft and a bush of sliding bearings, *J. Frict. Wear*, 2017, vol. 38, no. 3, pp. 242–251. https://doi.org/10.3103/s1068366617030163

12. Miler, D., Škec, S., Katana, B., and Žeželj, D., An experimental study of composite plain bearings: the influence of clearance on friction coefficient and temperature, *Strojniški Vestn.*, 2019, vol. 65, no. 10, pp. 547–556. https://doi.org/10.5545/sv-jme.2019.6108

Translated by Sh. Galyaltdinov